Thin-Walled Structures 85 (2014) 71–80

Contents lists available at ScienceDirect

Thin-Walled Structures

journal homepage: www.elsevier.com/locate/tws

An experimental study on clinched joints realized with different dies

F. Lambiase *, A. Di Ilio

Department of Industrial and Information Engineering and Economics, University of L'Aquila, via G. Gronchi 18, Zona Industriale di Pile, 67100 (AQ), Italy

ARTICLE INFO

Article history:
Received 6 September 2013
Received in revised form
13 July 2014
Accepted 8 August 2014

Keywords:
Joint Strength
Mechanical fastening
Failure mode
Clinching
Shear testing
Joining

ABSTRACT

An experimental investigation has been conducted on mechanically clinched joints, produced with fixed and extensible dies with different forming forces. Mechanical testing involving single lap shear tests, both with one and two joining points, and peeling tests were conducted under quasi-static conditions to assess the different mechanical behaviors of these joints. The effect of the processing conditions on the main mechanical response of the joints, namely the maximum strength, stiffness and absorbed energy, was investigated.

The results showed that the joints produced with the extensible die exhibited a similar strength as compared to those produced with the fixed die in single lap shear tests, while they are characterized by a higher strength (up to 40%) when loaded during the peeling test because of a larger interlock. In addition, the employment of extensible dies allows a drastic reduction of the forming loads as compared to those required by adopting the fixed dies.

1. Introduction

The mechanical fastening of thin structures is receiving considerable attention since it has the possibility of overcoming several problems concerning welding processes. Indeed, the increasing employment of high specific strength materials, such as aluminum alloys and high strength steels, in the automotive and aerospace fields and the difficulty in welding aluminum components, due to the natural presence of surface oxide layers, high conductivity and low melting point, has induced investigations into new fastening processes, generally based on mechanical joining. Conventional mechanical fastening processes requiring a predrilled hole are unsuitable for the automotive industry because of the high run time. Thus, self-pierce riveting and mechanical clinching are being more and more employed in order to reduce the fastening time of sheet components.

In mechanical clinching, the sheets are connected without the employment of subsidiary material but rather by generating a mechanical interlock between the sheets. The relatively simplicity of clinching tools, low cost of the machines, cleanness of the process, absence of surfaces pre-treatments, cleaning requirements as well as the reduced processing time (which is almost 1 s) represent the main benefits over competitive processes. Driven by such advantages, mechanical clinching has been also applied to relatively thick plates [1] and it has been extended to materials other than metals [2–4]. In order to improve the mechanical strength of clinched connections, clinching tools should be designed to produce high values of interlocks (between the sheets) without excessively reducing the neck thickness of the punch-sided sheet. In order to perform the tools optimization and increase the process robustness, FE models represent a viable solution [5].

Extensive literature on the static and dynamic strength of clinched joints has been produced [6–11]. The main joint failure mechanisms have been established in [12] while an analytical model to predict the mechanical strength of clinched joints during tensile tests on H-type specimens was proposed in [13]. The effect of process parameters has been intensively investigated to increase the clinched joints' strength produced with fixed [13,14] as well as extensible dies [15–17]. Because of the complex material flow during the joining operations, a series of studies has been carried with FE models [6,8,18,19] and optimization approaches have been developed for the automatic design of clinching tools [20–22]. Recent developments in employment of FE models to clinching processing deal with the prediction of the damage initiation and evolution in clinched connections [23,24], the improvement of the clinched connection quality by reducing the protrusion depth [25] and even the optimization of the machine design [26] to achieve the desired rigidity.

The aim of the current study is to experimentally assess the influence of the processing conditions and die type on the joint strength, the failure mode, the stiffness and the energy absorbed. Different mechanical tests were developed including single lap shear tests with one and two joints and peeling tests. The different failure modes arising in the tests were correlated to the geometry

* Correspondence to: Monteluco di Roio, 67040 (AQ), Italy.
Tel.: +39 0862 434422; fax: +39 0862 434303.
E-mail address: francesco.lambiase@univaq.it (F. Lambiase).

http://dx.doi.org/10.1016/j.tws.2014.08.004
0263-8231/

of the clinched joint according to the different processing conditions. In order to analyze the strain localization during the tests, a digital image correlation (DIC) technique was also employed.

The results show that the mechanical properties of clinched joints produced with extensible dies have a similar strength to that of joints produced with fixed dies during shear tests. Conversely, clinched joints produced with extensible dies exhibit a superior strength and absorb more energy than the joints produced with fixed dies when subjected to peeling forces. The results also showed that a lower forming force is required to join the sheet when extensible dies are employed.

Table 1
Mechanical properties of AISI 1005.

E [GPa]	$R_{p0.2}$ [MPa]	R_m [MPa]	E_{tot} [%]
203	167	307	33

Table 2
Chemical composition of AISI 1005.

C [%]	Mn [%]	P [%]	S [%]	Fe [%]
0.05	0.3	0.035	0.05	Remain

2. Materials and methods

2.1. Clinching tests

Experimental tests of clinch joining were performed on low-carbon steel AISI 1005 sheets with nominal thickness $t=1.0$ mm. The mechanical behaviors (measured from uniaxial tensile tests) and the chemical composition of the analyzed material are summarized in Tables 1 and 2, respectively.

The samples used for clinching tests were cut from a unique sheet. Clinching tests were performed using a portable JURADO machine, model Python, which can supply up to 30 kN. An extensible die and fixed dies were investigated, the former is a conventional extensible die supplied with the clinching machine which is suitable for ductile metals while the fixed dies were designed by the authors and produced by CAMS (Chieti, Italy). The three fixed dies have different shoulder diameters, while all the other characteristics are almost identical to the extensible die geometry. The diameter of the fixed dies ranges within the minimum diameter (before joining) and the maximum diameter (after joining) assumed by the extensible die. Indeed, the smaller die (FD1) has a diameter $D=6.1$ mm, which is a little larger than that of the extensible die before clinching. The larger die (FD3) has a diameter $D=6.7$ mm which produces a similar punch–die cavity volume to the extensible die when the joint is produced with the maximum load of 30 kN. In addition a further fixed die (FD2), having an intermediate diameter $D=6.4$ mm, was employed. The geometrical dimensions of the clinching tools are represented in Fig. 1.

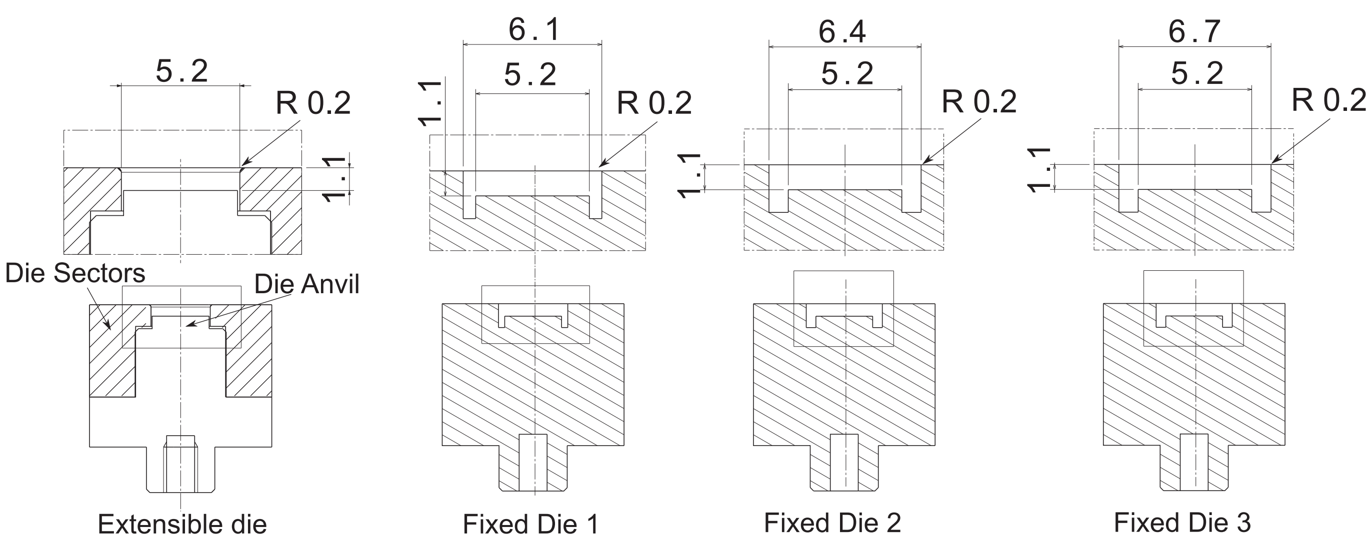

Fig. 1. Schematic of clinching tools with extensible and fixed dies.

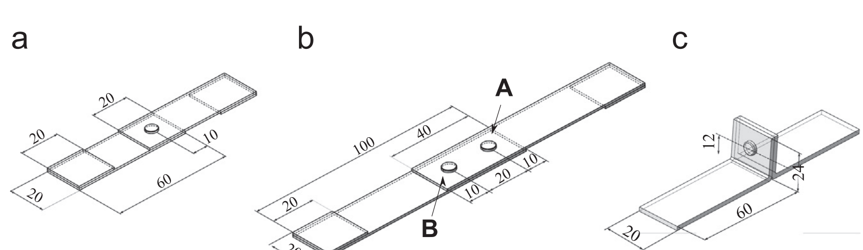

Fig. 2. Schematic of (a) single lap shear sample with one joint, (b) single lap shear sample with two joints and (c) peeling sample with one joint.

2.2. Geometrical and mechanical characterization of clinched samples

The main failure modes of clinched joints are button separation (unbuttoning), neck fracture or a combination of both mechanisms [13]. The occurrence of one of such failure modes depends on the geometrical characteristics of the clinch profile and the local strength of the material. In order to analyze the different mechanical properties of joints produced under different processing conditions, dimensional analysis was conducted and the main geometrical dimensions of the joints were measured. The samples were sectioned and the clinched joint profile was measured by means of an optical microscope, model LEICA DMI 5000M.

Single lap shear tests with single and double joints and peeling tests were carried out to analyze the different behaviors of the clinched joints produced with the extensible and fixed dies. For each processing condition three samples were tested. Fig. 2 shows the dimensions of the sample used in the shear lap tests with one and two joining points and peeling tests.

The tests were conducted at room temperature using a universal MTS 322.31 testing machine with 25 kN full scale load at a constant cross head speed of 2 mm/min until the complete separation of the sheets. The force displacement curve was recorded at a low sampling rate (5 sps) due to the low-speed rate of the test. Three replicates for each processing conditions were recorded. For each test, the main mechanical characteristics of the load–displacement curve, i.e., maximum strength P_{max}, absorbed energy E_n and the joint stiffness K (as depicted in Fig. 3), were analyzed.

In order to measure the strain distribution during the single lap shear test with two joints, DIC analysis was performed. The employment of DIC analysis is based on the correlation and tracking of different states of the sample during the tests in order to calculate the relative displacement of the tracked points/speckles. The great flexibility and robustness of such a technique has allowed the measurement of the strain distribution during mechanical testing of different types of joints produced on different materials [27–32]. Indeed, since the strain fields qualitatively reflect the stress distribution [27], the DIC analysis can help to discern the contribution of the two joints during the test. Therefore, for each test, a layer of white paint and a random spray pattern were applied to the sample surface prior to the shear test; thus, a sequence of images was acquired during the tests at a 1 Hz sampling rate.

A series of preliminary tests was conducted to determine a sound-processing window for the further analysis: a minimum force (22 kN) was adopted, since this was the minimum value, which allowed production of a sound joint using the extensible die. On the other hand, a value of 30 kN was assumed as the maximum force (which is the maximum load recommended by the punch manufacturer). A further intermediate value of 26 kN was also adopted resulting in a 3 (levels of force) × 4 (types of die) experimental plan.

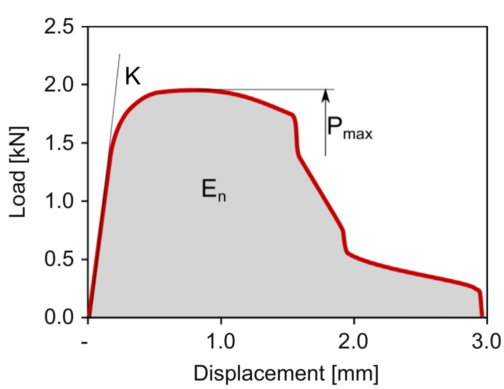

Fig. 3. Main mechanical behaviors measured during the tests.

3. Results and discussion

3.1. Joinability and geometric characterization of the joint profile

Regardless of the joining force, the larger fixed die, FD3, failed to produce the mechanical interlock between the sheets, as did the

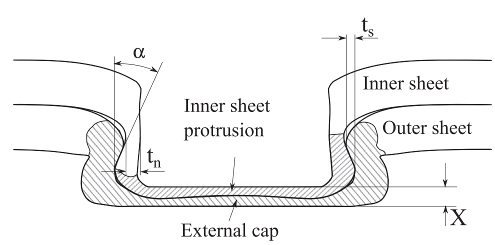

Fig. 5. Main geometric behaviors of clinched joints.

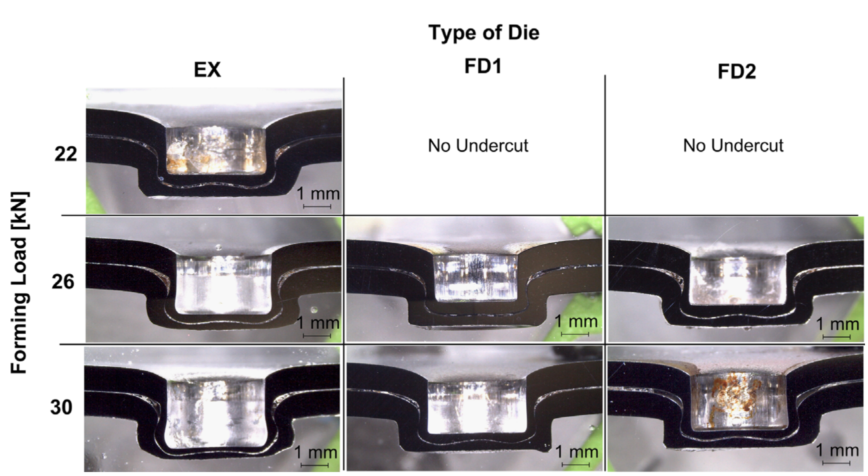

Fig. 4. Cross sections of clinched joints with different dies and forming loads.

other fixed dies FD1 and FD2, while these dies failed when using the minimum value of force (22 kN). Geometrical analysis was performed on the joints produced under the remaining processing conditions.

Fig. 4 depicts the cross sections of the clinched joints; as can be seen, the joints produced with the extensible die were significantly different from those produced with the two fixed dies. Although values of the neck thickness t_n of the joints produced with the different types of dies were relatively similar (ranging between 0.28 and 0.35 mm), the joints produced with the extensible dies were characterized by a larger interlock t_s (which in some cases was more than double compared to that produced with the fixed dies) and a lower residual base thickness X, which can be attributed to a lower hydrostatic stress in the cavity volume (because of the lower constraining effect produced by the sliding die shoulders). The joints produced with the extensible dies were characterized by a higher angle α, as depicted in Fig. 5, which plays an important role in the mechanical resistance of the clinched joints, influencing the failure mode [13]. Indeed, when the extensible dies are utilized the material comprised between the punch and the die anvil flows radially [15] leading to large values of α; on the other hand, the fixed dies exert a higher radial constraint which promotes the material flow towards the die groove resulting in smaller angles α.

Regardless of the type of die utilized, the increase in the forming force induced an increase in the interlock (as depicted in Fig. 6) and the α-angle, and a negligible reduction of the neck thickness. Nevertheless, the increase of the interlock with the forming load was only marginal in clinched joints produced with the fixed dies. In any case, the neck thickness to interlock ratio (which affects the failure mode) ranged between 1.8 (for high forming loads) and 7.1 (for low values of the forming load).

Additional tests were performed using the same punch stroke, to compare the cross sections of clinched connections with the same value of the protrusion thickness X. Fig. 7 depicts the cross sections of clinched connections having $X=0.6$ mm as well as the values for the interlock t_s and neck thickness t_n. As can be observed, the joint produced with the extensible die exhibits the highest value of

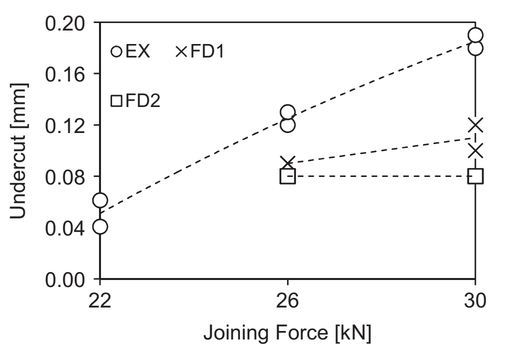

Fig. 6. Influence of joining force on interlock for joints produced with different types of dies.

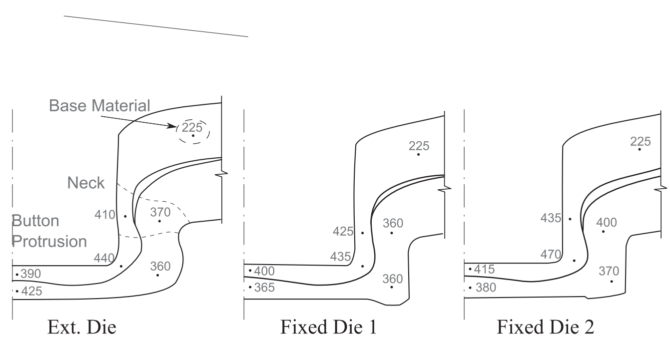

Fig. 8. Micro-hardness measurements performed on joints produced with different dies with $X=0.6$ mm.

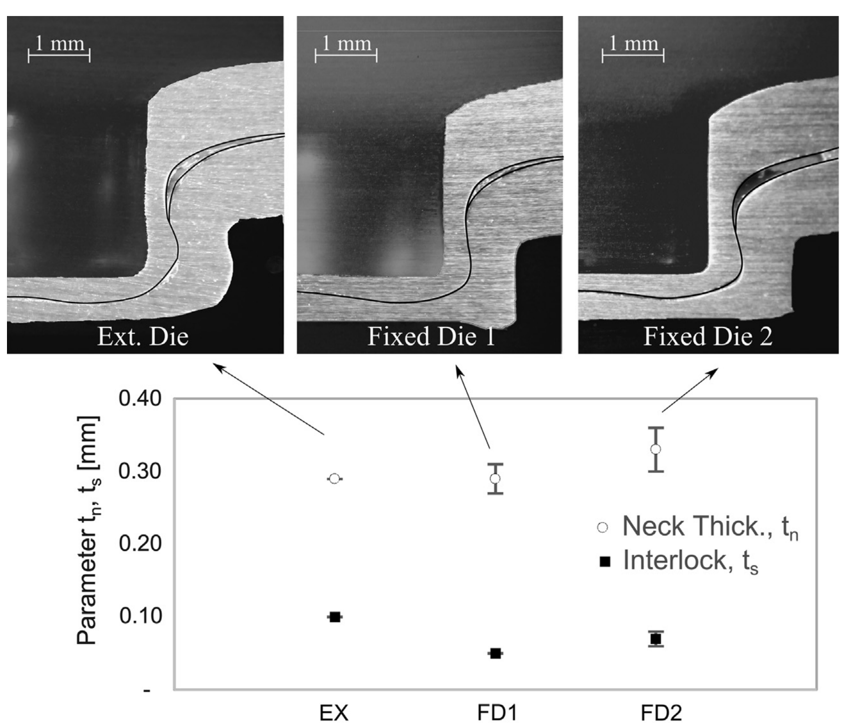

Fig. 7. Cross-sections and quality criteria of joints produced with the same X-parameter: $X=0.6$ mm.

interlock (t_s=0.10 mm) and a similar neck thickness (t_n=0.29 mm) as the joint produced with the fixed die FD1 (t_n=0.29 mm) that is characterized by a relatively low value of interlock (t_s=0.05 mm). On the other hand, the joint produced with the FD2 showed the highest value of neck thickness (t_n=0.33 mm) and an intermediate value of interlock (t_s=0.07 mm).

Micro-hardness tests were performed at specific locations, namely the joint neck and the button protrusion to compare the influence of the dies on the material flow. Fig. 8 depicts the micro-hardness for the above mentioned joints having the same value of X=0.6. The micro-hardness of the base material was 225 $HV_{0.1}$. As can be noted, the hardness of the clinched connections was increased by the work-hardening resulting from the large plastic deformation. For all the analyzed specimens, the highest value of micro-hardness was shown at the neck of the punch-sided sheet as well as at the bottom protrusion corner whereas the value of the micro-hardness was almost double as that of the base material. The die-sided sheets were characterized by a minor increase in micro-hardness indicating a minor material flow. Actually, while the punch-sided sheet is more constrained during the offsetting phase with a high localization of plastic deformation at the tool tip corner, during this phase the die-sided sheet almost undergoes to bending deformation. Comparing the micro-hardness values of joints produced with different dies it is shown that the flow stress is more sensitive to the different regions of the joint cross sections rather than the type of die. Indeed, the maximum difference in micro-hardness tests performed on the same regions of joints produced with different dies was lower than 7%.

3.2. *Test results of single lap shear test with one joint*

Fig. 7(a) and (b) shows the behavior of clinched joints produced with extensible and fixed dies, respectively, where it is possible to identify the typical stages of load bearing. First, a linear part up to point 1 relates to the elastic regime. As the displacement increases, the inner sheet protrusion tends to rotate out of the plane of loading direction (secondary bending) resulting in a reduction of the joint stiffness. However, this effect is much more evident in joints produced with the fixed dies which are characterized by a lower value of the interlock and then are much freer to rotate. Conversely, the joints produced with the extensible die, after the secondary bending, undergo a bearing of the clinch protrusion that will carry the whole load. The stress concentrates on a section of the inner sheet protrusion leading to a catastrophic failure of the joint. Indeed, a main crack nucleates at the base of the protrusion (point 3), which results in a steep reduction in the load carrying ability. Then, a more gentle decrease in load carrying ability is exhibited at point 4 of Fig. 7(a) during the propagation of the crack towards the center of rotation of the protrusion. Further displacement comes with significant rotation of the inner protrusion around the fulcrum, which still links the protrusion to the sheet leading to an almost constant load. As point 6 is reached, the complete separation of the protrusion from the sheet takes place, which results in a sudden drop of the carrying load until the complete loss of mechanical resistance.

The behavior of the clinched joints produced with the fixed dies is also characterized by an initial elastic regime after which a secondary bending takes place, as depicted in Fig. 7(b). However, on this kind of joint, the secondary bending is much more prolonged showing a plateau from point 2; indeed, because of the small interlock within the clinched joint, the inner sheet protrusion is much freer to rotate within the external cap (shown in Fig. 5). As the deformation continues up to point 3 the inner protrusion is gradually pulled out from the cap, which results in an almost constant load carrying capacity. As point 3 is reached, a crack nucleates and propagates, as occur in samples joined with extensible dies. On the other hand, in the joints produced with the larger die FD2, the separation of the sheets occurred by unbuttoning with or without a partial crack developing from the top head of the protrusion.

A summary of the mechanical performance of clinched joints in single lap shear single joint tests is presented in Fig. 7(c). The best performances in terms of shear strength and absorbed energy were achieved by clinched joints produced with the fixed die FD2, followed by those produced with the fixed die FD1 and those produced with the extensible die. A possible explanation could be related to the large interlock and α-angle, as those produced with the extensible die, which would result in higher stiffness of the joint with lower secondary bending and higher stress concentration that promotes early crack development of the joint.

The influence of the forming load on the mechanical behaviors of the clinched joints produced with the extensible die is negligible, while, on the other hand, an increase in the absorbed energy was observed on the clinched joint produced with the fixed dies. Such an increase could be attributed to the increase in the contact length between the inner protrusion and the external cap, which determined a prolonged unbuttoning effect.

The main failure modes on clinched joints subjected to shearing stress are summarized in Fig. 8. Failure mode a and b, also referred to as full shear and partial shear, mainly occurred on samples joined with the extensible and FD1 dies, respectively. Indeed, the joints with as large an interlock and α-angle as those produced by the extensible die are characterized by higher stiffness which results in full shear arising at the base of the joint protrusion. On the other hand, the failure mode b is prevalent on joints produced with the FD1 matrix. Indeed, in this case, the samples are characterized by a smaller interlock and α-angle. Herein, the internal protrusion initially slips on the ‘top hat’ internal surface inducing a significant detaching of the sheets. The detaching effect comes with an increase in the arm formed by the contact force and the internal sheet up to the nucleation of a crack, which develops from the base of the protrusion and propagates in the fulcrum direction.

Failure modes reported in Fig. 8(c) and (d) were referred to as unbuttoning with crack and full unbuttoning, respectively. These kinds of failure modes were observed on joints produced with the FD2 die, which is characterized by a larger punch–die cavity volume. Indeed, in this case, the interlock is smaller than that produced with the FD1 die; therefore, during the detaching of the sheets, any nucleation of the crack takes place at the base of the protrusion. Nevertheless, during the detaching of the sheets the contact force localizes on the top of the protrusion, which may lead to a crack nucleation just in that place.

3.3. *Test results of single lap shear test with two joints*

Fig. 9(a) and (b) shows the load–displacement curves of single lap double joint samples produced with the extensible and the fixed dies, respectively. The difference between the shear strength of the samples produced with the extensible die and fixed dies has been drastically reduced from that observed in the single joint samples. Indeed, comparing the results of shear tests concerning single and the corresponding double joint samples it emerges that, when using the extensible die, the maximum strength of the sample with two joints is almost 100% higher than that of the corresponding single joint. On the other hand, the shear strength measured in single lap shear tests of samples with two joints produced with the fixed die is only 60% higher than that of the corresponding single joint. This can be ascribed to the secondary bending which is much more reduced in the two-joint

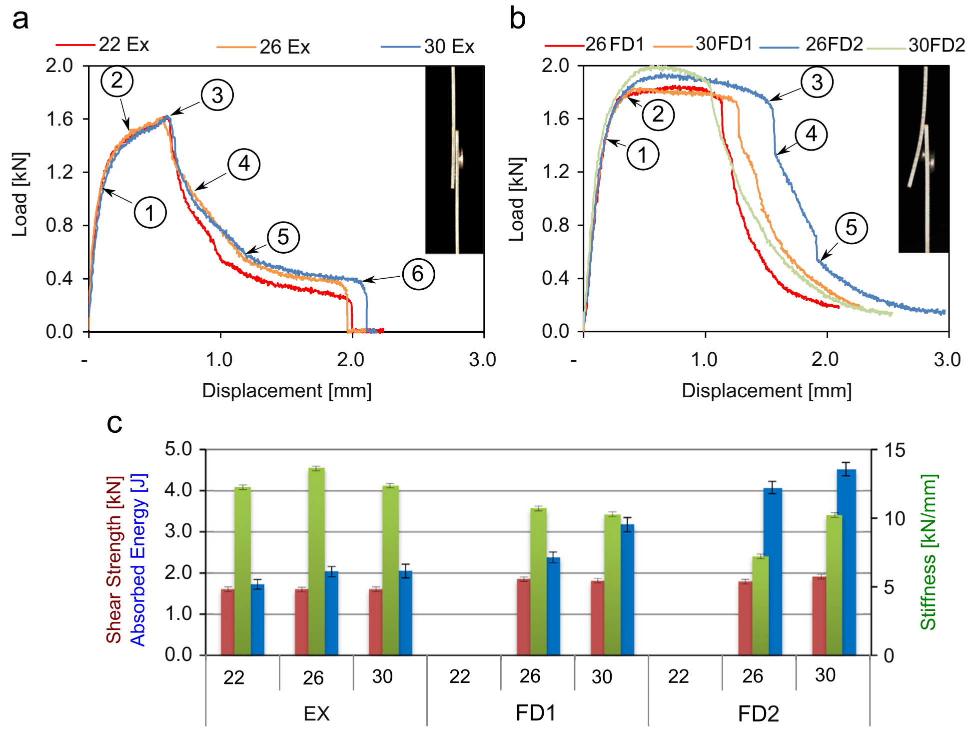

Fig. 9. Lap shear load curves for specimens produced with different forces with (a) extensible die and (b) fixed dies.

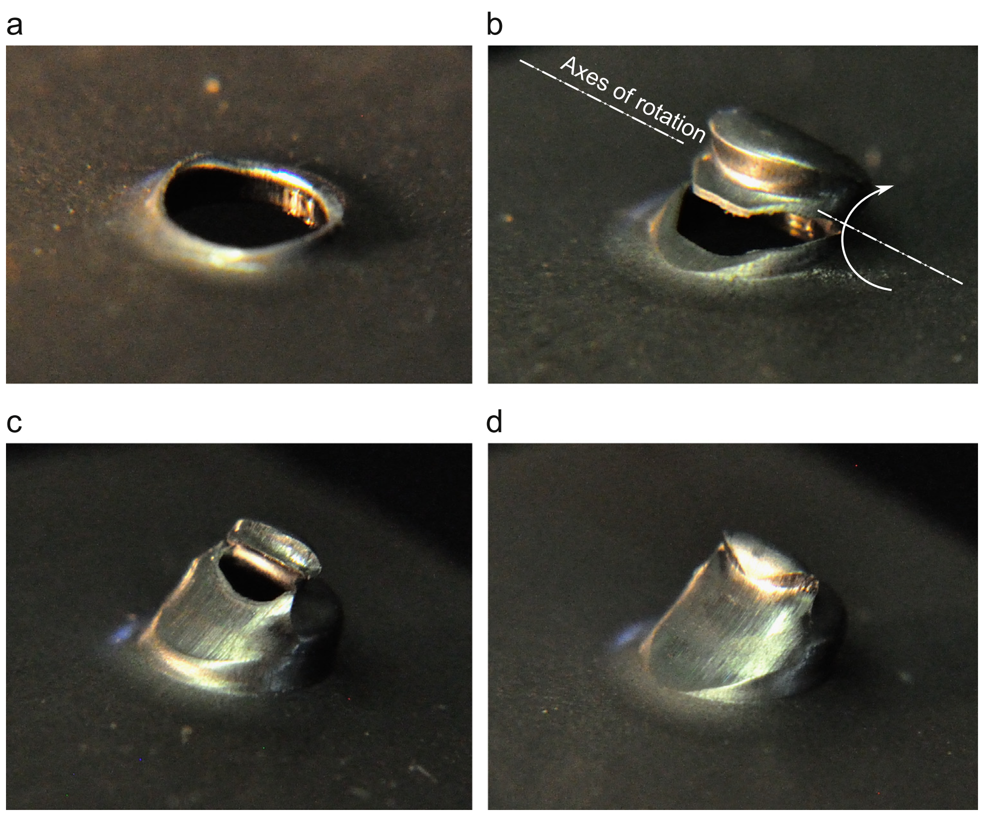

Fig. 10. Main failure modes of clinched joints during shear test: (a) full shear; (b) half shear; (c) unbuttoning with crack and (d) full unbuttoning.

configuration and thus penalizes the strength of double joint samples produced, joined with the fixed dies.

From a further comparison with the results of shear tests with one joint, it emerges that the displacement at which the peak of load occurs seems to be almost unaffected by the number of joints, while a significant increase in the stiffness (which almost doubles) is achieved. In addition, as it occurs for the single lap single joint tests, the shear strength seems to be only slightly influenced by the joining load.

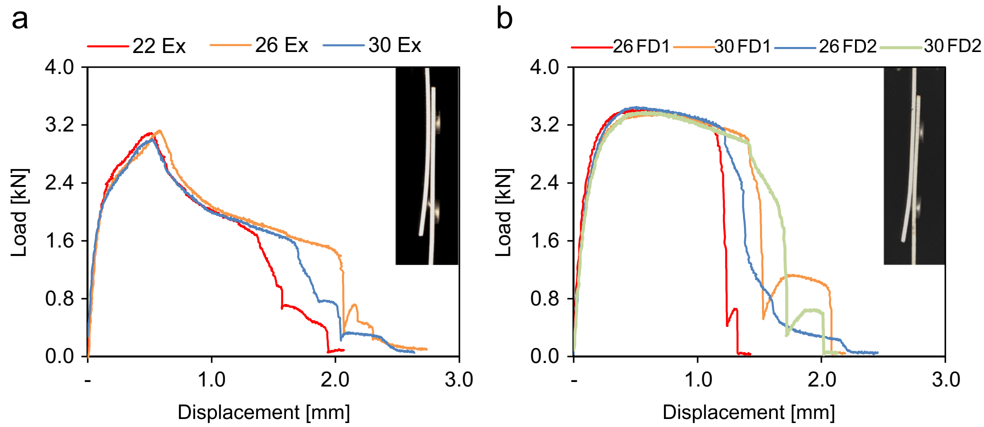

Fig. 11. Double lap shear load extension curves for specimens produced with different forces with (a) an extensible die; (b) fixed dies.

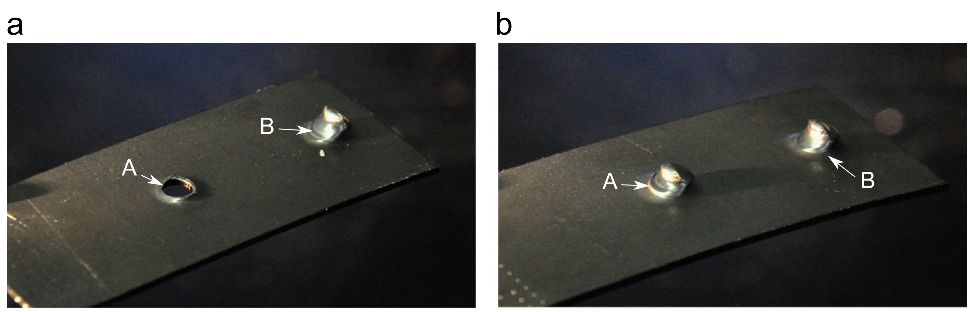

Fig. 12. Failure modes of sheet samples in the single lap shear test with two joints produced with (a) the extensible die and (b) the fixed dies.

During all the tests on this kind of sample, the two joints (referred to as A and B in Fig. 2) behaved differently. Indeed, after the first linear-elastic part, whereas the two joints work concurrently, the detaching effect starts in correspondence with joint A.

The main failure modes of the sample used in the single lap shear test with two joints are reported in Fig. 10. It was observed that the samples produced with the extensible die were characterized by failure mode a on the A-joint and failure mode b on the B-joint (except that joined with the maximum force failed by full shear), as illustrated in Fig. 10(a). On the other hand, the samples joined with the fixed dies were mainly characterized by failure mode b on the A-joint and failure mode d on the B-joint, as illustrated in Fig. 10(b).

In order to discern the contribution of the two joints during the test, DIC analysis was performed during testing of the samples joined with different types of dies. Fig. 11 shows the typical behavior of a single lap shear sample with two joints achieved with the extensible (a) and fixed die (b). The sequence of pictures corresponds to the points in the load–displacement curves.

The samples joined with the extensible and fixed dies showed similar trends in the first two steps, namely linear-elastic regime and secondary bending.

Conversely, for larger displacements, a high difference in the mechanical behavior of the samples joined with different dies can be appreciated. Indeed, while in samples joined with the extensible die the load just before the peak increases rapidly, in the other kind of joints a much more gentle increase can be observed. Probably, in the joints produced with the extensible dies, a higher strain hardening occurs before the nucleation of the crack because of the high constraining conditions, which characterize this kind of joint. On the other hand, in the samples joined with the fixed dies, the larger secondary bending comes with a more gentle increase in the load.

The in situ analysis of strain by the DIC technique has also allowed the contribution of the two joints (A and B) during the tests to be discerned. In the first step, the two joints almost work simultaneously, as demonstrated by the uniform distribution of the strain; however, as secondary bending begins, strain localizes at the joint A. In the samples joined with the extensible die, after the maximum force is reached, a crack nucleates and develops at the A-joint with a consequent sudden drop of the load (point 3); thus the load is sustained more uniformly by the two joints. Further displacement determines crack nucleation and development also at joint B, as also confirmed by the strain analysis; in fact, the strain is concentrated at the top side of the two joints (point 4). The load decreases almost linearly up to point 5 then a drastic drop in the load is exhibited because of the failure of joint A.

Different behavior was observed in samples joined with the fixed dies. Indeed, as the maximum force was reached, a gentle decrease in the load was noted, indicating the nucleation of a crack at joint A. DIC analysis also confirms the loss of carrying load capacity by joint A. However, because joint B is less constrained by bending (it will separate by unbuttoning failure modes c or d), the load decreases more gradually up to the complete failure of joint A (point 5).

3.4. Test results of peeling test

Fig. 12(a) and (b) shows the load–displacement curves registered during peeling tests on samples joined with the extensible and fixed dies respectively. During the test, different phases can be appreciated. First, the load increases almost linearly; then a more gentle increase of the load occurs (because of the plastic bending of the sheet) up to reaching a peak load. Although the samples produced with different dies behaved almost similarly up to the

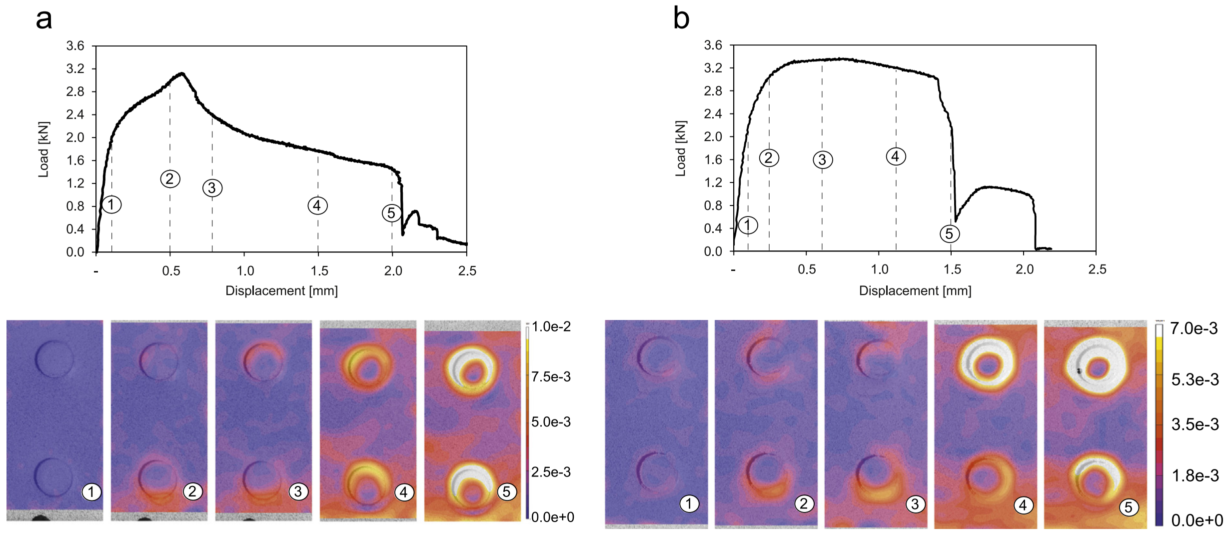

Fig. 13. Evolution of strain distributions measured by DIC on double shear lap joints produced with the extensible die (a) and the fixed die FD1 (b).

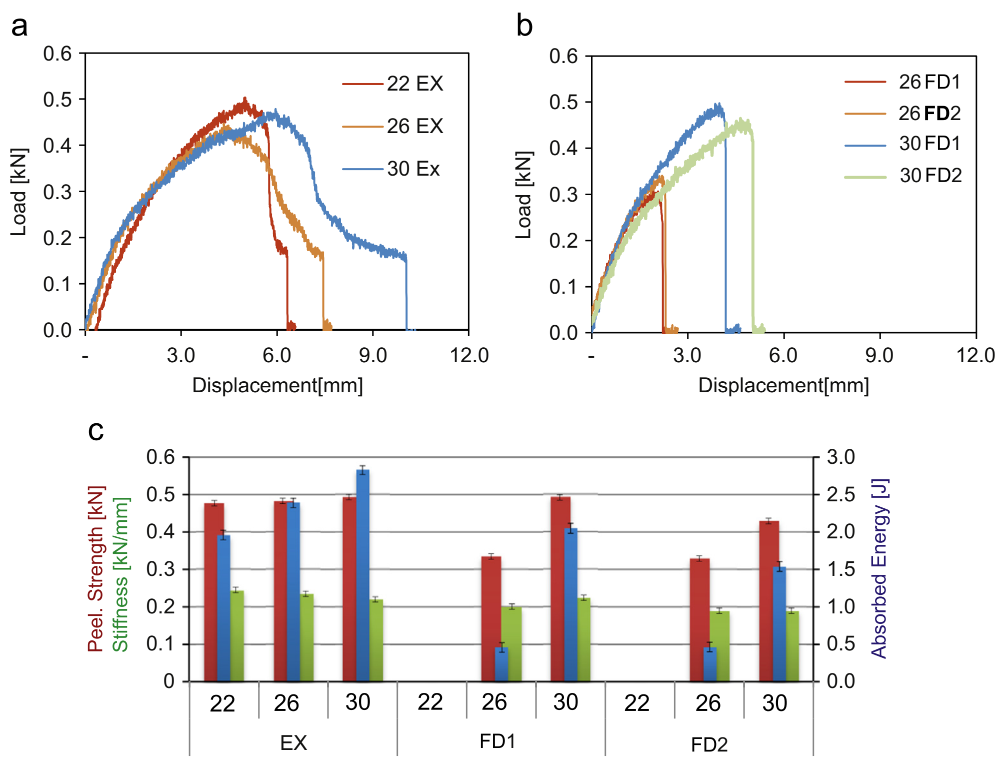

Fig. 14. Peeling load extension curves for specimens produced with different forces with an (a) extensible die; (b) fixed dies.

peak load, a relative difference between the load–displacement curves of the samples joined with the two kinds of dies affected the behavior of the joint after the load peak because of the different failure modes. Indeed, samples joined with the extensible die failed by partial necking that resulted from early neck thinning and then the joint separated by unbuttoning. During neck thinning, a crack develops and propagates from the side of the joint near the loaded side, thus inducing a gradual decrease of the force. In this kind of sample, after the peak load, the mechanical interlock is gradually reduced up to almost zero which causes the complete separation of the sheet by unbuttoning.

The samples joined by the fixed dies failed by unbuttoning; therefore, after the peak, the load reduced to zero almost immediately because of the sudden separation of the sheet as shown in Fig. 13.

The influence of the process conditions on the main mechanical behaviors is presented in Fig. 14(c).

As can be seen, the extensible die allowed a relatively high strength to be produced with the lowest forming load of 22 kN. Referring to samples joined with the extensible die, it appears that the influence of the forming load was almost negligible on the joint strength. This is probably due to the mechanism of failure. Indeed, because of the relatively large value of the interlock and the large α-angle, the joint failed by partial necking that is influenced by neck thickness. On the other hand, the samples joined with the fixed dies benefited from higher joining, since larger interlocks were obtained.

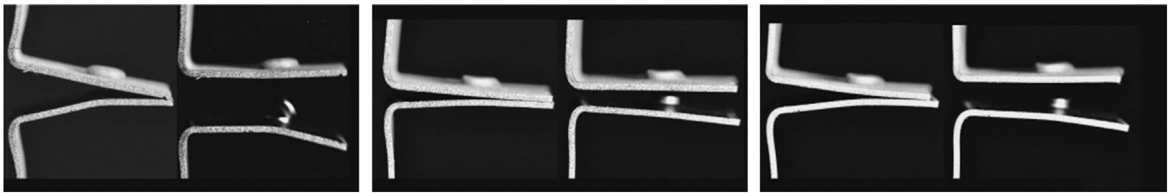

Fig. 15. Side view of samples before and after the complete separation of the sheets. (a) 30 EX, (b) 26 F2 and (c) 30 F2.

In this kind of sample also the absorbed energy benefited from a larger interlock and then a higher joining force.

Because of the different failure mechanisms, the joints produced with the extensible dies were characterized by higher absorbed energy as compared to those produced with the fixed dies. The large interlocks produced with the extensible die induce a large bending of the sample during the peeling test, as also confirmed by Fig. 15. On the other hand, because of the much smaller values of the interlock, the joints produced with the fixed dies were characterized by a much lower value of absorbed energy. In addition, the complete separation of the sheets (Fig. 15) occurred for much smaller values of displacement, as illustrated in Fig. 15 (a) and (b).

4. Conclusions

An experimental test campaign was conducted to assess the main differences among clinched joints produced with different die configurations, including an extensible die and three different fixed dies. The samples were joined with different forming forces and were analyzed by means of different mechanical tests, including lap shear tests, with one and two joints, and peeling tests. Digital Image Correlation was also utilized to analyze the strain distribution at the joints neighbors during mechanical tests. In addition, geometrical analysis of the cross sections was performed in order to understand the different behaviors of the samples during the tests. The main results are reported as follows:

- a minor joining force is required to produce sound joints when extensible dies are used despite of fixed/grooved dies;
- the employment of extensible dies allow producing large interlocks which result in an increase in strength and absorbed energy of joints during peeling tests;
- the joints produced with the extensible die were stiffer than those produced with the fixed dies because of the larger α-angle and interlock. This geometrical characteristic also affected the failure mode of such joints that mainly developed by crack nucleation and propagation;
- the joints produced with the fixed dies mainly failed by unbuttoning because of smaller interlocks and α-angles;
- the joints produced with the fixed dies are characterized by the highest strength and absorbed energy when loaded in the lap shear test with one joint.

Acknowledgments

The authors would like to thank Jurado, Rivotosto di Assisi (Italy) for providing the part of the experimental equipment utilized in the research. The authors would also like to thank CAMS, Chieti (Italy) for the manufacturing of customized clinching dies.

References

[1] Israel M. The suitability of analytical and numerical methods for developing clinching processes with thick sheet metal. Adv Mater Res 2014;907: 151–63.
[2] Lüder S, Härtel S, Binotsch C, Awiszus B. Influence of the moisture content on flat-clinch connection of wood materials and aluminium. J Mater Process Technol 2014;214:2069–74.
[3] Lee C-J, Lee J-M, Ryu H-Y, Lee K-H, Kim B-M, Ko D-C. Design of hole-clinching process for joining of dissimilar materials – Al6061-T4 alloy with DP780 steel, hot-pressed 22MnB5 steel, and carbon fiber reinforced plastic. J Mater Process Technol 2014.
[4] Gerstmann T, Awiszus B. Recent developments in flat-clinching. Comput Mater Sci 2014;81:39–44.
[5] Drossel WG, Falk T, Israel M, Jesche F. Unerring planning of clinching processes through the use of mathematical methods. Key Eng Mater 2014;611–612:1437–44.
[6] Coppieters S, Lava P, Hecke RV, Cooreman S, Sol H, Houtte PV, Debruyne D. Numerical and experimental study of the multi-axial quasi-static strength of clinched connections. Int J Mater Form 2012;6:437–51.
[7] Kim H-K. Fatigue strength evaluation of the clinched lap joints of a cold rolled mild steel sheet. J Mater Eng Perform 2012.
[8] Mori K, Abe Y, Kato T. Mechanism of superiority of fatigue strength for aluminium alloy sheets joined by mechanical clinching and self-pierce riveting. J Mater Process Technol 2012.
[9] Mucha J, Witkowski W. The experimental analysis of the double joint type change effect on the joint destruction process in uniaxial shearing test. Thin-Walled Struct 2013;66:39–49.
[10] Mucha J, Witkowski W. The clinching joints strength analysis in the aspects of changes in the forming technology and load conditions. Thin-Walled Struct 2014;82:55–66.
[11] He X, Zhao L, Yang H, Xing B, Wang Y, Deng C, Gu F, Ball A. Investigations of strength and energy absorption of clinched joints. Comput Mater Sci 2014.
[12] Varis J. Ensuring the integrity in clinching process. J Mater Process Technol 2006;174(1–3):277–85.
[13] Lee C-J, Kim J-Y, Lee S-K, Ko D-C, Kim B-M. Design of mechanical clinching tools for joining of aluminium alloy sheets. Mater Des 2010;31(4):1854–61.
[14] Mucha J. The analysis of lock forming mechanism in the clinching joint. Mater Des 2011;32(10):4943–54.
[15] Lambiase F, Di Ilio A. Finite element analysis of material flow in mechanical clinching with extensible dies. J Mater Eng Perform 2013;22(6):1629–36.
[16] Lambiase F. Influence of process parameters in mechanical clinching with extensible dies. Int J Adv Manuf Technol 2013.
[17] Gibmeier J, Rode N, Lin Peng R, Oden M, Scholtes B. Residual stress in clinched joints of metals. Appl Phys A Mater Sci Process 2002;74(0):s1440–2.
[18] Coppieters S, Cooreman S, Sol IH, Debruyne1 ID. Reproducing the experimental strength of clinched connections with finite element methods. Paper presented at the SEM annual conference & exposition on experimental and applied mechanics. 2007.
[19] He X. Recent development in finite element analysis of clinched joints. Int J Adv Manuf Technol 2010;48(5–8):607–12.
[20] Oudjene M, Benayed L, Delameziere A, Batoz J. Shape optimization of clinching tools using the response surface methodology with Moving Least-Square approximation. J Mater Process Technol 2009;209(1):289–96.
[21] Lambiase F, Di Ilio A. Optimization of clinching tools by means of integrated FE modeling and Artificial Intelligence Techniques. Procedia CIRP 2012;12:163–8.
[22] Roux E., Bouchard P.O. (2013) Kriging metamodel global optimization of clinching joining processes accounting for ductile damage. J Mater Process Technol.
[23] Zhao SD, Xu F, Guo JH, Han XL. Experimental and numerical research for the failure behavior of the clinched joint using modified Rousselier model. J Mater Process Technol 2014.
[24] Xu F, Zhao SD, Han XL. Use of a modified Gurson model for the failure behaviour of the clinched joint on Al6061 sheet. Fatigue Fract Eng Mater Struct 2014;37(3):335–48.

[25] Wen T, Wang H, Yang C, Liu LT. On a reshaping method of clinched joints to reduce the protrusion height. Int J Adv Manuf Technol 2014.
[26] Markowski T, MUCHA J, Witkowski W. FEM analysis of clinching joint machine's C-frame rigidity. Maint Reliab 2013;15:51–7.
[27] Li D, Han L, Thornton M, Shergold M. Influence of edge distance on quality and static behaviour of self-piercing riveted aluminium joints. Mater Des 2012;34:22–31.
[28] Heimbs S, Schmeer S, Blaurock J, Steeger S. Static and dynamic failure behaviour of bolted joints in carbon fibre composites. Compos Part A Appl Sci Manuf 2013;47:91.
[29] Abibe AB, Amancio-Filho ST, dos Santos JF, Hage E. Mechanical and failure behaviour of hybrid polymer–metal staked joints. Mater Des 2013;46:338–47.
[30] Leitão C, Costa MI, Khanijomdi K, Rodrigues DM. Assessing strength and local plastic behaviour of welds by shear testing. Mater Des 2013;51:968–74.
[31] Daiyan H, Grytten F, Andreassen E, Osnes H, Lyngstad OV. Numerical simulation of low-velocity impact loading of a ductile polymer material. Mater Des 2012;42:450–8.
[32] Leitão C, Galvão I, Leal RM, Rodrigues DM. Determination of local constitutive properties of aluminium friction stir welds using digital image correlation. Mater Des 2012;33:69–74.